

Observation of Saturn-Ring Defects around Solid Microspheres in Nematic Liquid Crystals

Yuedong Gu and Nicholas L. Abbott*

Department of Chemical Engineering, University of Wisconsin, 1415 Engineering Drive, Madison, Wisconsin 53706

(Received 24 March 2000)

We report an experimental system based on rigid, monodisperse, microparticles with tunable surface properties for the study of topological defects that form about dispersed solid phases in anisotropic media. We clearly observe equatorial Saturn-ring defects to form a distance $(0.09 \pm 0.01)R$ from the surface of isolated microspheres (with strong homeotropic anchoring) dispersed in nematic phases. These defects, some of which are observed to be stable for up to a month, are similar in size to past theoretical predictions (with strong homeotropic anchoring) and can be reversibly expanded in an electric field.

PACS numbers: 61.30.Jf, 61.30.Gd, 64.70.Md, 83.70.Jr

Topological defects are ubiquitous in materials as diverse as crystalline solids and liquid crystalline composites. They are of broad relevance to condensed matter physics [1]. Topological defects in nematic liquid crystals (LCs) arise when mechanical stresses associated with continuous variations of the orientation of the LCs (director) are relieved by the localized loss of nematic order within the LCs [2]. Several past experimental studies have reported the introduction of isotropic liquid microdroplets into uniformly aligned nematic LCs (nematic emulsions) to be accompanied by the formation of topological defects around the liquid droplets. The topological defects appear to mediate anisotropic forces that act between the droplets and thus can lead to unusual ordering of ensembles of liquid droplets [3–6]. The topological defects can also mediate forces between liquid droplets and confining surfaces [7]. This type of LC-mediated anisotropic force, unlike electrostatic or van der Waals forces, has not been examined widely [1,3–11].

Past experimental studies have largely focused on the structure of topological defects formed about microdroplets of isotropic solutions ($1\text{--}10\ \mu\text{m}$ in diameter) of surfactant and polymer dispersed in thermotropic liquid crystals [3–5]. Isolated liquid microdroplets with homeotropic (normal to surface) anchoring conditions suspended in aligned films of nematic LCs are generally observed to be accompanied by hyperbolic hedgehog defects (a dipolar point defect) [3]. This hyperbolic hedgehog has been calculated by using theory to correspond to a free energy minimum [1,12]. Terentjev and his colleagues, however, have predicted that an equatorial Saturn ring could also correspond to a free energy minimum [7,9–11] and, recently, Poulin and his colleagues have observed a dark line to pass across the diameters of microdroplets with inferred weak homeotropic anchoring conditions and suggested that it may correspond to a Saturn-ring defect [13]. These experiments, however, did not reveal the position of the defect relative to the surface of the microdroplet, nor was it known if the defect passed entirely around the equator of the droplet. We report here an experimental investigation of topological defects formed about solid microspheres with well-defined and

uniform surface properties. Using this model system with strong homeotropic surface anchoring conditions, we are able to provide unambiguous evidence for the existence of Saturn-ring defects that are displaced from the surface of the microspheres by a distance of $\sim 0.1R$ and that completely encircle the microspheres at their equator [7,9–13]. The sizes of the Saturn-ring defects are found to be in good agreement with theory and can be reversibly expanded by application of an external electric field.

The experimental system that we report is based on micrometer-sized glass spheres coated with thin films of gold. The surfaces of the gold-coated spheres are derivatized by the chemisorption of alkanethiols that cause homeotropic anchoring of LCs. We believe the experimental system we report here to be a useful one for several reasons. First, the size (or sizes) and shapes of the microparticles can be precisely specified for the study of both spherical and anisometric particles in LCs. Second, the anchoring of LCs on monolayers of alkanethiols on planar gold surfaces has been investigated in a number of past studies [14–16]. Experimental conditions leading to planar, tilted, or homeotropic anchoring are well established and can be reliably reproduced over long periods of time (months) [15,16]. It is also known that the lateral mobility of the alkanethiols is low and thus contact of the spheres with the LCs will not result in a redistribution of these species on the surface of the spheres (and thus position-dependent anchoring energies on the surface of the spheres). Third, because the treated glass spheres are rigid, the spheres cannot coalesce and fuse. This makes it possible to study topological defects over long periods of time (months) as well as the organization of ensembles of particles formed under the influence of attractive interactions. It is also possible to observe the structure of defects formed about clusters of particles. Fourth, it is possible to study systems containing mixtures of particles that possess different yet stable and well-defined anchoring conditions.

We prepared our experimental system by first spreading monodisperse glass spheres (40, 60, or $100\ \mu\text{m}$ in diameter, SPI Supplies) on a Petri dish. The spheres were coated with a total of $\sim 15\ \text{\AA}$ Cr ($5\ \text{\AA}/\text{sec}$) and then $\sim 60\ \text{\AA}$ Au

(1 Å/sec) by sputtering [17]. In order to ensure a uniform coverage of gold over the entire surface of the spheres, gold was deposited in eight steps (7–8 Å per step). At the end of each step, the spheres were collected in a small bottle, vigorously shaken, and then redispersed on the Petri dish. The gold-coated spheres were then immersed into ethanolic solutions of $\text{CH}_3(\text{CH}_2)_9\text{SH}$ and $\text{CH}_3(\text{CH}_2)_{15}\text{SH}$ (0.85 and 0.15 mM, respectively) for at least 2 h so as to form self-assembled monolayers (SAMs) on the surface of the gold. The mixed SAMs are known to cause homeotropic anchoring of nematic 5CB (4-cyano-4'-pentylbiphenyl) [16]. We observed topological defects around the SAM-treated spheres by using capillary action to draw a mixture of 5CB (heated into its isotropic phase) and spheres into a LC cell with known anchoring conditions. The parallel surfaces of the LC cells were formed from glass microscope slides coated with thin films of gold that were derivatized with SAMs formed from $\text{CH}_3(\text{CH}_2)_{14}\text{SH}$. Self-assembled monolayers formed from $\text{CH}_3(\text{CH}_2)_{14}\text{SH}$ on obliquely deposited films of gold are known to lead to planar anchoring [15,16,18]. The surfaces of the cells were spaced apart by thin films of Mylar. Here we confine our observations to the topological defects formed about isolated spheres. We define "isolated spheres" to be those spheres that are at least three diameters away from their nearest neighbor.

We observed the optical appearance of the LCs near the spheres using a polarized-light microscope with the analyzer removed. When a mixture of 40 and 100 μm (in diameter) microspheres with homeotropic anchoring was placed in a $\sim 120\text{-}\mu\text{m}$ -thick LC cell, the equatorial planes of 40 μm spheres with Saturn rings were observed to be on the same focal plane (within $\sim 10\ \mu\text{m}$) as those of 100 μm spheres, as evidenced by a series of confocal microscopy images at various focal planes. From this result, we conclude that the surface of the 40 μm sphere is $40 \pm 20\ \mu\text{m}$ from the closest surface of the LC cell. Elastic forces mediated by the LC act between the sphere and the LC cell surface to prevent gravitational sedimentation of the sphere close to the LC cell surface [7].

As shown in Fig. 1(a), we report optical images of a sphere at three focal planes. Figures 1(b)–1(f) show images of a gold-coated sphere (100 μm in diameter) hosted within a LC cell with planar anchoring on the cell surfaces. The thickness of the cell was $\sim 120\ \mu\text{m}$. The continuity of the Saturn ring about the sphere suggests that the sphere did not contact the surfaces of the LC cell in our experiments. Unambiguous evidence of off-surface Saturn rings was also recorded for 40 μm spheres in a $\sim 120\text{-}\mu\text{m}$ -thick cell (see above). To maximize the details of the Saturn ring that can be seen in the figures presented in this Letter, we show here images of the Saturn ring formed about a 100 μm sphere in a $\sim 120\text{-}\mu\text{m}$ -thick LC cell. With the focus near plane 1, an apparent disclination line perpendicular to the far-field bulk director was observed [Fig. 1(b)]. As the focus was moved down to

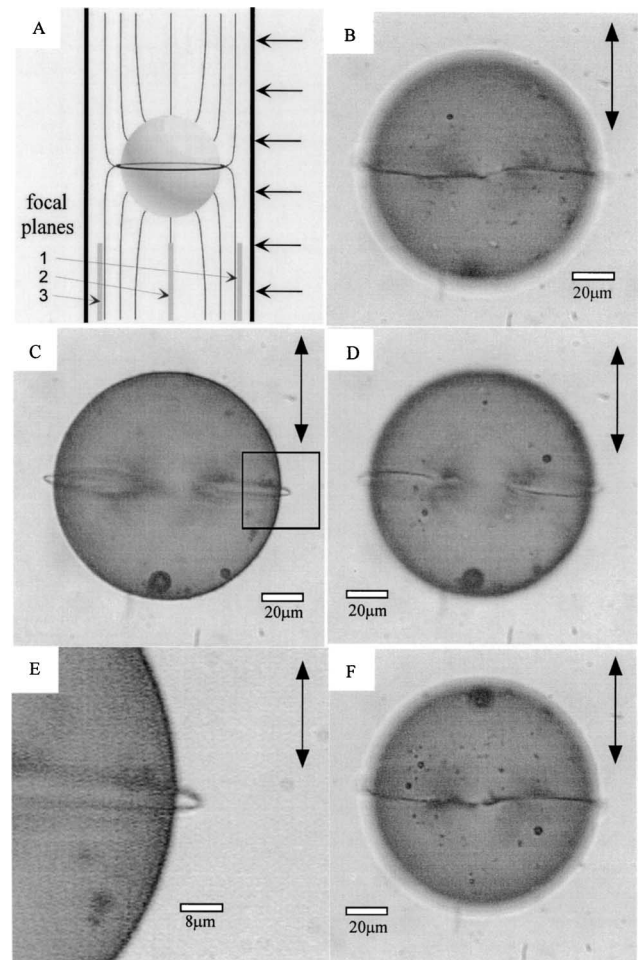


FIG. 1. Optical appearance of nematic LCs observed near an isolated sphere on which the LCs were anchored homeotropically. The LCs and sphere were sandwiched between two parallel surfaces on which the LCs were anchored in a planar orientation. (a) Schematic illustration of an isolated sphere within the LC cell. The six arrows indicate the direction of observation of the LCs, and the three arrows indicate the focal planes at which images were recorded. The theoretical near-surface director profile (thin lines) and the equatorial disclination ring (thick line) are shown. (b)–(f) Optical images of a gold-coated sphere (100 μm in diameter) in a $\sim 120\text{-}\mu\text{m}$ -thick LC cell. The double-headed arrows in each figure indicate the orientation of the bulk LCs. Images on focal planes 1, 2, and 3 are shown in (b), (c), and (d), respectively. (f) is the optical image on focal plane 3, viewed in a direction that is opposite to the six arrows in (a). (e) is an enlarged image of the boxed area in (c). The images were obtained without the use of the analyzer in a polarized-light microscope.

plane 2, two off-surface curvilinear disclination lines on either side of the sphere were in sharp focus [Fig. 1(c)]. An enlarged image of the boxed area in Fig. 1(c) is shown in 1(e). Although, the disclination line appeared to be discontinuous at the focal plane 3 [Fig. 1(d)], when the image on this plane was examined from the other side of the cell (turning over the cell), the disclination line was continuous [Fig. 1(f)]. These results, when combined, are consistent with the presence of a line disclination that runs around the

equator of the sphere (a Saturn-ring defect). We observed Saturn-ring defects around some particles to be stable for over one month.

When using LC cells with planar anchoring, we measured the radii, a^* , of the Saturn rings to be $(1.093 \pm 0.009)R$ and $(1.091 \pm 0.005)R$ for 40 and 100 μm (diameter) spheres, respectively, in a $\sim 120\text{-}\mu\text{m}$ -thick LC cell, and $(1.095 \pm 0.003)R$ for a 60 μm (diameter) sphere in a $\sim 70\text{-}\mu\text{m}$ -thick cell, where R is the radius of the spheres. Several theoretical methods have been used in the past to predict the radii of Saturn rings around spheres with homeotropic boundary conditions in aligned nematic phases. The first study predicted $a^* \approx 1.25R$ by proposing a minimal free energy *ansatz* (possible director profile) that satisfied all symmetry, boundary, and far-field director requirements [10]. With a similar method, Lubensky *et al.* obtained a value of $a^* \approx 1.08R$ [1]. The second approach used a Monte Carlo simulation and the method of simulated annealing with a Metropolis sampling criterion. This method predicted $a^*_{\text{max}} \approx 1.10R$ for strong homeotropic anchoring on sphere surfaces [11]. Even though the simulations involve a number of approximations (such as assuming a single elastic constant to describe the distortion of the nematic phases), the past theoretical predictions and our experimental observations show close agreement. We note that the elastic constants K_{11} , K_{22} , and K_{33} (splay, twist, and bend, respectively) for 5CB are within a factor of 2 of each other near room temperature [19].

We applied an electrical potential difference (ac, 50 Hz) across a $120\text{-}\mu\text{m}$ -thick LC cell containing 100 μm spheres by using the gold films of the LC cell as electrodes. The anchoring on the surfaces of the LC cells was planar. We observed that the radii of the Saturn rings increased as the voltage difference applied across the cell was ramped from 0 to 3 V [Figs. 2(a)–2(c)]. The electric field-induced expansion of the ring was reversed upon reduction of the applied field [Fig. 2(d)]. Similar results were obtained for 60 μm spheres in $\sim 70\text{-}\mu\text{m}$ -thick cells. The conducting surface of the gold-coated sphere defines an equipotential contour at the surface of the sphere. The direction of the electric field is normal to the equipotential contour, and the LC molecules align in this direction because of their molecular dipole moment [20,21]. The near-surface electric field promotes a director profile normal to the surface of the sphere. This effect likely causes an expansion of the near-surface radial hedgehog alignments and thus an expansion of Saturn-ring radius a^* .

We also observed some spheres in the LC cells to be surrounded by topological defects that did not correspond to Saturn rings. Most of them were observed to possess a single topological defect at either one of their poles, and thus they possessed dipolar symmetry (Fig. 3). Some of the defects possessing dipolar symmetry came from spontaneous transformation of Saturn-ring defects. Dipolar point defects (hyperbolic hedgehogs) have been reported

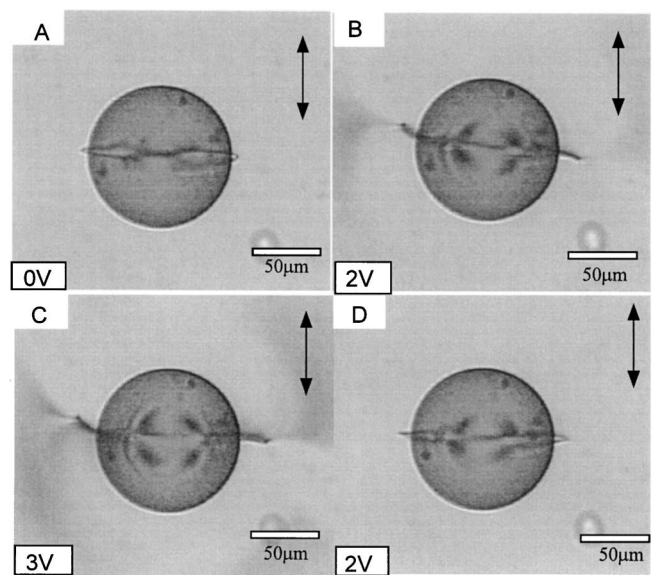


FIG. 2. Reversible, electric field-induced expansion of a Saturn-ring defect about a gold-coated sphere with homeotropic boundary conditions. The LCs and sphere were sandwiched between two parallel surfaces on which the LCs were anchored in a planar orientation. The diameter of the sphere was 100 μm , and the thickness of the cell was $\sim 120\text{ }\mu\text{m}$. The arrow in each figure indicates the orientation of the bulk LCs prior to application of the electric field. (a) No external electric field, 0 V. (b) Applied voltage of 2 V. (c) Applied voltage of 3 V. (d) Optical appearance of the LCs after the applied voltage was decreased from 3 to 2 V. The images were obtained in a polarized-light microscope with the analyzer removed.

in past studies to form about droplets of aqueous surfactant and polymer solutions. Although the defects in Fig. 3 are dipolar, they are not obviously point defects. High resolution images of some defects reveal a complex defect structure that looked like a crumpled line (“ball of string”). We refer to this type of topological defect as a dipolar defect.

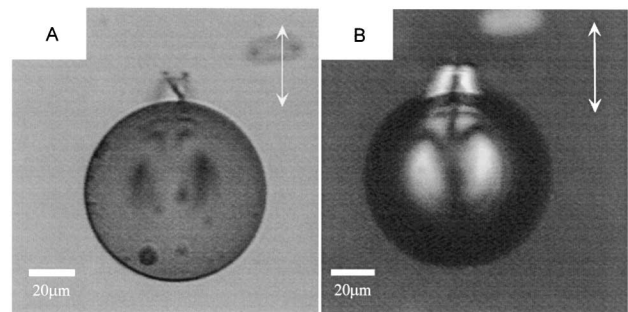


FIG. 3. Optical image of a sphere with a single defect at one of the poles of the sphere. The radius of the sphere was 100 μm and the thickness of the LC cell containing the sphere was $\sim 120\text{ }\mu\text{m}$. The anchoring of the LCs was homeotropic on the surface of the sphere and was planar on the surfaces of the LC cell. The arrows indicate the orientation of the bulk LCs. The image in (a) was obtained in a polarized-light microscope with the analyzer removed. The image in (b) was obtained with crossed polars.

We also measured the influence of the strength of homeotropic anchoring on the defect structures formed about the microspheres by using mixed SAMs of $\text{CH}_3(\text{CH}_2)_9\text{SH}$ and $\text{CH}_3(\text{CH}_2)_{15}\text{SH}$ that possessed systematically different compositions. As the homeotropic anchoring at the surface of the microspheres was weakened, there was no significant change in the population of dipolar and Saturn-ring defect structures. When the homeotropic anchoring became sufficiently weak, neither Saturn rings nor dipolar defects were observed. These results contrast to those reported by Poulin and co-workers using inverted nematic emulsions [13].

The experimental system that we report for the study of topological defects is based on microspheres that possess uniform surface chemistry defined by the covalent bonding of organized monolayers of molecules to the surfaces of the spheres. By using surface chemistry that leads to the anchoring of nematic phases of 5CB in a homeotropic orientation on the surfaces of the microspheres, we observed the formation of Saturn-ring topological defects in the LC. The measured radii of the Saturn rings agree with past theoretical predictions of the size of Saturn-ring defects [1,10,11] and can be manipulated reversibly by application of electric fields. Past studies based on liquid microdroplets have observed linear clusters of microdroplets to form under the influence of dipolar, long-range attractive, and short-range repulsive forces acting among the droplets [3–5]. Because the Saturn-ring defect has quadrupolar symmetry, interparticle forces that result from the defect are qualitatively different from those due to formation of dipolar defects around isotropic liquid droplets dispersed in liquid crystals [1,3–9]. Recently, it has been reported that nanometer-sized latex particles with homeotropic boundary conditions, unlike microdroplets of surfactants and polymers, aggregate along an angle off the director [13]. This type of organization is suggestive of a quadrupolar interaction. This type of interaction, however, cannot be studied in nematic emulsions because the droplets coalesce upon contact. Our ability to systematically manipulate the orientations of liquid crystals at the surfaces of the solid particles by tuning the structures of self-assembled monolayers formed on the surfaces [14–16,20] provides a general experimental system to study the organizations of microparticles under the influence of forces mediated by liquid crystals. In preliminary observations, for example, we have observed Saturn-ring defects to encircle clusters

of microspheres with homeotropic anchoring. When combined with the demonstrated capability to expand the Saturn rings by using an electric field, we believe the experimental system reported in this Letter may open new ways to approaches by which interparticle forces can be placed under active control.

We gratefully acknowledge support by the Camille and Henry Dreyfus Foundation, the Office of Naval Research, and the Materials Research Science and Engineering Center Program of NSF under Award No. NSF-DMR 9632527. We also thank the Keck Neural Imaging Laboratory for providing access to a confocal microscope.

*Author to whom correspondence should be addressed.

Email address: abbott@engr.wisc.edu

- [1] T. C. Lubensky, D. Pettey, N. Currier, and H. Stark, *Phys. Rev. E* **57**, 610 (1998).
- [2] P. G. de Gennes and J. Prost, *The Physics of Liquid Crystals* (Clarendon, Oxford, 1993), 2nd ed.
- [3] P. Poulin and D. A. Weitz, *Phys. Rev. E* **57**, 626 (1998).
- [4] P. Poulin, V. Cabuil, and D. A. Weitz, *Phys. Rev. Lett.* **79**, 4862 (1997).
- [5] P. Poulin, H. Stark, T. C. Lubensky, and D. A. Weitz, *Science* **275**, 1770 (1997).
- [6] R. B. Meyer, *Mol. Cryst. Liq. Cryst.* **16**, 355 (1972).
- [7] E. M. Terentjev, *Phys. Rev. E* **51**, 1330 (1995).
- [8] H. Stark, J. Stelzer, and R. Bernhard, *Eur. Phys. J. B* **10**, 515 (1999).
- [9] R. W. Ruhwandl and E. M. Terentjev, *Phys. Rev. E* **55**, 2958 (1997).
- [10] O. V. Kuksenok *et al.*, *Phys. Rev. E* **54**, 5198 (1996).
- [11] R. W. Ruhwandl and E. M. Terentjev, *Phys. Rev. E* **54**, 5198 (1996).
- [12] H. Stark, *Eur. Phys. J. B* **10**, 311 (1999).
- [13] O. Mondain-Monval *et al.*, *Eur. Phys. J. B* **12**, 167 (1999).
- [14] V. K. Gupta and N. L. Abbott, *Phys. Rev. E* **54**, 4540 (1996).
- [15] W. J. Miller *et al.*, *Appl. Phys. Lett.* **69**, 1852 (1996).
- [16] R. A. Drawhorn and N. L. Abbott, *J. Phys. Chem.* **99**, 16511 (1995).
- [17] J. L. Vossen and W. Kern, *Thin-Film Processes* (Academic Press, New York, 1978).
- [18] J. J. Skaife and N. L. Abbott, *Chem. Mater.* **11**, 612 (1999).
- [19] D. Gu *et al.*, *Macromolecules* **24**, 2385 (1991).
- [20] V. K. Gupta and N. L. Abbott, *Science* **276**, 1533 (1997).
- [21] W. P. Parker, *Proc. Soc. Photo-Opt. Instrum. Eng.* **2689**, 195 (1996).